Synchrotron x-ray microdiffraction diagnostics of multilayer optoelectronic devices

Z. Cai, W. Rodrigues, P. Ilinski, D. Legnini, B. Lai, and W. Yun
Advanced Photon Source, 9700 S. Cass Avenue, Argonne, IL 60439 USA

E.D. Isaacs, K.E. Lutterodt, J. Grenko, R. Glew, S. Sputz, J. Vandenberg, R. People, M.A. Alam, M. Hybertsen, and L.J.P. Ketelsen
Bell Laboratories, Lucent Technologies, 700 Mountain Avenue, Murray Hill, NJ 07974 USA

State-of-the-art optical components for telecommunications, such as the electroabsorption modulator laser (EML) and the wavelength selectable laser array, require sophisticated integration of multiquantum well (MQW) lasers, modulators, and optical waveguides on different regions of the same wafer [1, 2]. Integration is possible in the quaternary alloys $In_{1-x}Ga_xAs_{1-y}P_y$ because of the metal-organic chemical-vapor deposition (MOCVD) technique of selective area growth (SAG) [1]. SAG works as follows: While the group III precursors (e.g., trimethyl gallium) in MOCVD readily bond to a free InGaAsP surface, they will not stick to a SiO_2 surface. Therefore, the layer of gas just above a thin oxide mask patterned onto the InGaAsP will be rich in the group III precursors. The group III precursors can then diffuse to the free-InGaAsP surface in the vicinity of the oxide where they may stick. This leads to an enhancement of the epitaxial growth rate relative to the field regions far from the oxide. By the appropriate choice of an oxide mask pattern, SAG allows precise control of the spatial variation of multilayer thickness, composition, and crystallographic strain on micron-length scales. While SAG is serving as a platform for an ever-widening variety of integrated optoelectronic devices, the details of the growth processes are still not well understood. SAG processes have been extensively characterized by standard techniques such as photoluminescence, transmission electron microscopy, and interferometry. However, because of the ultrasmall volume of material in the active regions of optoelectronic devices, direct x-ray characterization using standard sources is impossible. The only way to directly characterize as-grown devices with submicron resolution is with synchrotron-based x-ray microprobe techniques. Therefore, using the x-ray microdiffraction capabilities of an x-ray microprobe at the Advanced Photon Source (APS), we have measured the crystallographic strain and multilayer thickness of as-grown InGaAsP multilayer device material produced with SAG. Our principal result is that the growth enhancements are different for the well and barrier layers. Comparison of these surprising results with a recently developed vapor-phase diffusion model for SAG reveals that this can arise from different incorporation rates for the group III metals into the barrier and well materials, respectively. We also show that the spatial variations of SAG material in a fully processed device are continuous and smooth, which is an essential ingredient for monolithic device integration.

The x-ray microdiffraction results described here were obtained at the 2-ID beamline at the APS at Argonne National Laboratory [3]. A schematic of the 2-ID x-ray microprobe is shown in Figure 1. The principal components include a Si(111) double-crystal monochromator, microfocusing optics positioned 70 m from the undulator source, and a four-circle diffractometer with submicron XYZ sample positioning capability. The microfocusing optics consist of either a 5 μm pinhole or a phase zone plate with a 7 cm focal length that produce a beam size of 0.5 μm vertical x 1.0 μm horizontal with a flux of 1.5 x 10^{10} photons/s and for 11 keV x- rays. This represents a gain in flux of approximately 1250 over a pinhole with the same area (0.5 μm^2).

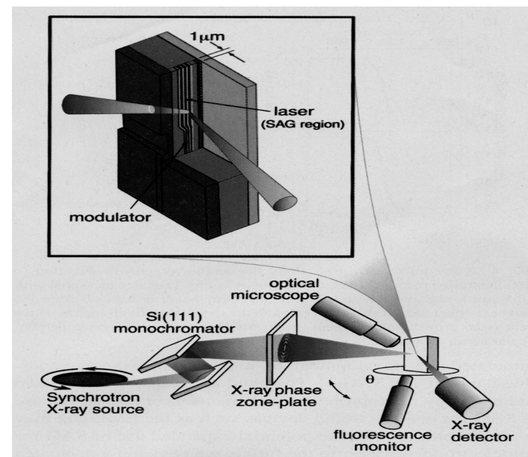

Figure 1: Schematic of x-ray microprobe beamline at the APS. Inset: schematic of a monolithically integrated InGaAsP multiquantum well electroabsorption modulator/laser device.

Bragg scans were measured by scanning the θ–2θ of the diffractometer. Imperfect centering of the sample and slight wobble of the θ axis could lead to some sample motion during a θ scan. However, this motion was held to less than the x-ray spot size with small active corrections of the sample position along the scattering vector (z axis) while monitoring Ga K-edge fluorescence with an energy-dispersive detector.

Figure 2 shows a series of microdiffraction scans measured with the 5 μm pinhole along the $\langle 001 \rangle$-growth direction in multilayer device material grown with SAG.

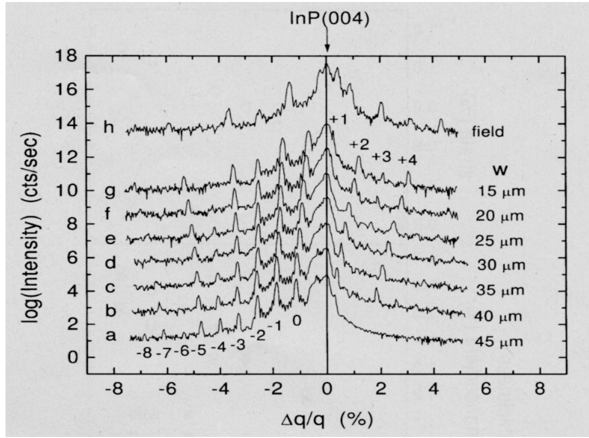

Figure 2: X-ray microdiffraction along the multilayer growth direction in device material produced using selective-area growth technique measured with a 5 µm pinhole. Each scan represents a different SAG mask width from (a) 45 µm to (g) 15 µm in steps of 5 µm. Curve (h) is in the field region far from the SAG mask.

The epitaxial growth consisted of seven quantum well periods buried beneath approximately 1 μm of InP and InGaAsP cap layers. The 11 keV x-rays easily penetrate the cap layers. The log of the intensity is plotted versus $\delta q/q_0 = \cot(\theta)\delta\theta$ in units of percent ($\times$ 100), where $\delta\theta = \theta - \theta_0$ is the diffractometer angle relative to the InP(004) Bragg angle (θ_0 = 22.58° at 11 keV) and $q_0 = 4\pi/[4d_{\text{InP}} \sin(\theta_0)]$. The vertically offset scans represent material grown with pairs of rectangular oxide masks [see the inset in Figure 3(c)] with increasing widths w from (a) 45 μm to (g) 15 μm in 5 μm steps all with 20 μm gaps. Each scan was measured at the center of the gap. The uppermost scan (h) was measured in the field region from the oxide masks. The principal features in Figure 2 are the InP(004) substrate Bragg peak (which saturates the detector) and the MQW superlattice peaks labeled by order (i.e., –2, –1, 0, 1,…). The position of the zeroth-order peak gives the average strain $(\alpha\perp - a_{\text{InP}})/a_{\text{InP}}$ perpendicular to the layers of the MQW, relative to the InP substrate (a_{InP} = 5.8687 Å). The separation between adjacent superlattice peaks is proportional to the inverse of the MQW period. The intrinsic widths and the presence of high-order superlattice peaks as well as the fringes between the superlattice peaks attest to the low defect density and sharpness of the MQW interfaces produced with SAG.

The well and barrier thickness and average perpendicular strain were determined by a simulation [4] of each of the curves in Figure 2. From the thickness, we determined the SAG thickness enhancements, t(SAG)/t(field), relative to the field region. These are summarized by the filled points in Figure 3. In the field region the average perpendicular strain was 0.185% and the thicknesses were t_w = 70 Å and t_b = 59 Å (w = well and b = barrier). In Figure 3(c), we plot the band gap measured with microphotoluminescence in the same devices and at the same positions as the microdiffraction measurements.

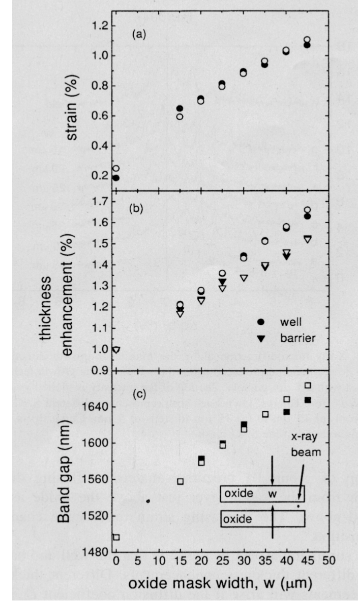

Figure 3: (a) Average perpendicular strain and (b) thickness enhancements for SAG device material determined from the diffraction measurements of Fig. 2. (c) Microphoto-luminescence determination of the band gap. The data are shown by filled points and the model in [7] by open points.

The monotonic increase in thickness enhancement with oxide mask width is due to the increasing buildup of group III precursor material diffusing during growth from the vapor layer just above the oxide as described. The increasing strain reflects the changing composition [5].

A surprising aspect of Figure 3 is that the well and barrier show different thickness enhancements. Different thickness enhancements will arise if the diffusion coefficient (D_V/κ) is different for the well and barrier materials. This implies that the growth rate constant (κ) is different for the well and barrier materials. In contrast, the mass transport coefficient (D_V) will be the same for both since it depends only on the reduced mass of the H_2 carrier gas. A three-dimensional vapor-phase diffusion model for SAG [6] recently developed for multilayers by People *et al.* [7] shows good agreement (open points in Figure 3) with the data with diffusion coefficients D_V/κ(In) = 22 μm and D_V/κ(Ga) = 135.8 μm for the well and D_V/κ(In) = 44.5 μm and D_V/κ(Ga) = 274.7 μm for the barrier. The model also shows good agreement with the measured band gap using the same diffusion coefficients. The shorter diffusion lengths for the group III precursors (larger κ) in the well means that the group III metal is more likely to stick, giving the larger thickness enhancement that we observe. While the three-dimensional vapor-phase model with different diffusion coefficients for well and barrier describes the data, it does not give insight into why κ should vary. The size of κ depends on the chemistry of dissociation of the group III metal from the precursor molecule. Therefore, it is not clear at this time how the rather small differences in the composition of the

vapor phase and free surfaces associated with well and barrier growth give rise to approximately a factor of two difference in κ.

In order to fully evaluate SAG as a means to large-scale optoelectronic device integration, it is essential to characterize fully processed devices. The latter stages of processing of the EML device leave an active mesa of MQW material which is approximately 1 μm wide (see the inset in Figure 1). Characterization of the narrow mesa required the higher spatial resolution provided by the zone plate described previously. Figure 4 shows a series of microdiffraction scans taken at regular intervals along the active mesa in a device grown with a 35 μm-wide SAG mask. In the insets, we plot the MQW period and average perpendicular strain, which clearly show that the MQW material varies smoothly from the laser to the modulator. This continuity of material is essential for monolithic device integration. Figure 4 also shows that the quality of the MQW material after processing is quite good (i.e., low defect density and sharp interfaces).

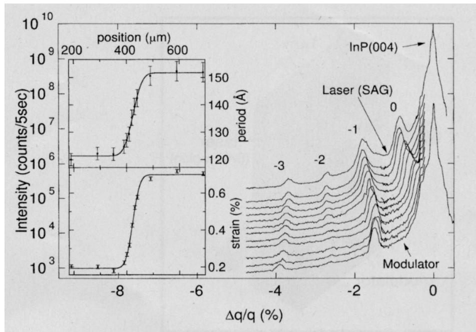

Figure 4: X-ray microdiffraction along the multilayer growth direction in a full processed EML (see the inset in Figure 1) device measured with a 0.5 μm x-ray spot. The position of the x-ray beam is scanned from thickness-enhanced MQW laser region to the modulator (field) region where there is no growth enhancement. Inset: MQW period and average perpendicular strain as a function of position.

In this report, we have described the application of an x-ray microprobe with 0.5 μm lateral resolution for nondestructive characterization of optoelectronic devices. In particular, by measuring the strain and multilayer thickness in device material grown by SAG we have learned the surprising fact that the well and barrier have different thickness enhancements. The success of these measurements has stimulated the development of a three-dimensional vapor-phase model for SAG [6].

Acknowledgments

The authors gratefully acknowledge J.E. Johnson and J. Maser. Use of the APS was supported by the U.S. Department of Energy, Basic Energy Sciences, Office of Science, under Contract No. W-31-109-Eng-38.

References

[1] E.J. Thrush, J.P. Stagg, M.A. Gibbon, R.E. Mallard, B. Hamilton, J.M. Jowett, and E.M. Allen, *Mater. Sci. Eng.,* B **21**, 130 (1993).

[2] T. Takiguchi, T. Itagaki, M. Takemi, A. Tekemoto, Y. Miyazaki, K. Shibata, Y. Hisa, K. Goto, Y. Mihashi, S. Takamiya, and M. Aiga, *J. Cryst. Growth* **170**, 705 (1997).

[3] W. Yun, B. Lai, D. Shu, A. Khounsary, Z. Cai, J. Barraza, and D. Legnini, *Rev. Sci. Instrum.* **67**, 3373 (1996). [SPIN] First citation in article.

[4] J.M. Vandenberg, D. Gershoni, R.A. Hamm, M.B. Panish, and H. Temkin, *J. Appl. Phys.* **66**, 3635 (1989).

[5] E.D. Isaacs, K. Evans-Lutterodt, M.A. Marcus, A.A. MacDowell, W. *et. al.*, *Diagnostic Techniques for Semiconductor Materials and Devices*, *Vol. 97-12*, (The Electrochemical Society, Pennington, NJ, 1997), 49.

[6] M.A. Alam, R. People, E.D. Isaacs, K. Evans-Lutterodt, T. Siegrist, T. Pernell, J. Vandenberg, S.K. Sputz, S.N.G. Chu, D.V. Lang, L. Smith, and M. Hybertsen, *Appl. Phys. Lett.* **74**, 2617 (1999).